TẠP CHÍ KHOA HỌC
TRƯỜNG ĐẠI HỌC SƯ PHẠM TP HỒ CHÍ MINH
Tập 20, Số 3 (2023): 386-399
Website: https://journal.hcmue.edu.vn
ISSN: 2734-9918

HO CHI MINH CITY UNIVERSITY OF EDUCATION
JOURNAL OF SCIENCE
Vol. 20, No. 3 (2023): 386-399
https://doi.org/10.54607/hcmue.js.20.3.3612(2023)

Research Article

A SEMI-TRANSPARENT COMPOSITE FILM FROM RICE STRAW-BASED MICROFIBRILLATED CELLULOSE AND CHITOSAN AND ITS APPLICATION IN LIGHT MANAGEMENT

Tran Van Khue[1], Le Van Thuan[2,3], Nguyen Minh Hiep[4], Dang Ngoc Sy[5], Doan Minh Thu[1], Le Hoang Sinh[1,2*]

[1]VNUK Institute for Research and Executive Education, The University of Danang, Vietnam
[2]Center for Advanced Chemistry, Institute of Research and Development, Duy Tan University, Vietnam
[3]The Faculty of Natural Sciences, Duy Tan University, Viet Nam
[4]Center of Radiation Technology and Biotechnology, Nuclear Research Institute, Da Lat, Vietnam
[5]Center of mechanical engineering, Duy Tan University, Viet Nam
[*]Corresponding author: Le Hoang Sinh – Email: sinh.le@vnuk.edu.vn
Received: October 11, 2022; Revised: November 08, 2022; Accepted: December 30, 2022

ABSTRACT

Semi-transparent composite film from rice straw-based microfibrillated cellulose and chitosan (MFC/CS) has been demonstrated to be a promising candidate light management material for the next generation optical engineering applications. Here, the lignin-modified MFC was prepared successfully through a green method, in which the MFC was first extracted using dilute sodium hydroxy solution on a homogenizer at 5000 rpm. The dissolved lignin was then deposited on the MFC surface by neutralizing it with a dilute hydrochloric acid solution. MFCs were obtained with diameters ranging from 2-5 μm and lengths up to 200 μm. Decoloration of lignin by removing its chromophore groups was conducted using peracetic acid treatment using a mixture of hydrogen peroxide and acid acetic with a volume ratio of 4:1. The MFC film shows good transparency and excellent diffusing effects with MFC/CS weight ratios of 1:3 and 1:1.

Keywords: green method; light management; microfibrillated cellulose; rice straw

1. Introduction

The increasing world population has caused a significant increase in global energy needs (Breyer, 2020; Eyl-Mazzega & Mathieu, 2020; Lee & Yang, 2019). The topic of energy efficiency in buildings has been considered a critical issue recently. Several innovative materials have been investigated and developed in the last decades for opaque and transparent elements, high-performant lighting systems, and more efficient heating and

Cite this article as: Tran Van Khue, Le Van Thuan, Nguyen Minh Hiep, Dang Ngoc Sy, Doan Minh Thu, & Le Hoang Sinh (2023). A semi-transparent composite film from rice straw-based microfibrillated cellulose and chitosan and its application in light management. *Ho Chi Minh City University of Education Journal of Science, 20*(3), 386-399.

cooling systems that maximize energy savings (Ascione et al., 2021; Fang et al., 2023; Rashidi et al., 2018; Song et al., 2018; Y. Sun et al., 2018; Tällberg et al., 2019; Z. Wang et al., 2020; Yang et al., 2022). Glass windows and doors have positively impacted the quality of the indoor environment since they provide an outdoor view and benefit from daylight. However, these glazed elements suffered from high thermal and solar sunlight transmittance inside a building. Therefore, glazing systems are important for building thermal and visual comfort, resulting in improved energy efficiency. Modern buildings tend to have large glazing areas; thus, conventional glazing leads to significant heat exchanges between the indoor and outdoor environments that can cause discomfort glare. Research and development in the field of glazing systems have experienced a rapid evolution with several innovative breakthroughs, which fall into three main approaches: (i) reduce heat exchange between indoor and outdoor environments; (ii) reduce solar transmittance of sunlight to an inside building; and (iii) promoting effective sunlight harvesting and offering comfortable indoor lighting. Applying solar control film/coating can reduce heat exchange between inside and outside environments. However, this film/coating can block the outdoor view or/and negatively impact the thermal environment of urban spaces (Mariano-Hernández et al., 2021; Mohelnikova, 2011; Pereira et al., 2019, 2022). The smart windows, including electro-, thermos-, mechano-, and photochromics, can optimize solar transmittance inside space. However, these systems are expensive and short-lived (Eh et al., 2018). Electrochromic need an electric system for operation. The development of new light management materials that can promote effective sunlight harvesting and offer comfortable indoor lighting has recently attracted much attention (Abuelnuor et al., 2018; Jiang et al., 2022; Xia, Chen, Li, et al., 2021). Previous studies reported a scalable, transparent wood for promoting effective sunlight harvesting and offering comfortable indoor lighting (Dong et al., 2022; Mi et al., 2020; J. Sun et al., 2022; K. Wang et al., 2023; K. Wang, Liu, et al., 2022). However, this method is a limited kind of wood and wood pattern. Cellulose nanopaper (CNP), assembled from cellulose nanofibrils, has emerged as a newly-developed optical functional material due to its fascinating light management capabilities, which are high transparency and tunable built-in transmittance haze, high thermal and UV stability, intrinsic sustainability, and biodegradation (Jiang et al., 2022; Li et al., 2021; K. Wang, Zhang, et al., 2022; Zhao et al., 2021). Cellulose nanofibrils can be synthesized by hydrolysis delignified lignocellulosic resources using high concentration sulfuric acid (e.g., 60-65 wt%). The wastewater from this process can cause serious problems to the environment. Lignin, a complex amorphous aromatic polymer, serves as the essential surrounding matrix of cellulose microfibrils in natural plants and provides mechanical support, water transport, and bacterial defense for the plant. With UV-absorbing, amphiphilic, thermoplastic, antioxidative, and antimicrobial, lignin can act as a functional cementing agent for cellulose nanofibrils to form densified nanopaper matrices with high UV-shielding, water and thermal

stability, and durable performance (Jiang et al., 2019; Lizundia et al., 2021; Xia, Chen, Yao, et al., 2021). For this reason, lignin-containing cellulose nanopaper, or lignocellulose nanopaper (LNP), has attracted much attention recently (Djafari Petroudy et al., 2019; Jiang et al., 2020; Oliaei et al., 2020; Zhang et al., 2020). Unfortunately, lignin's inherent light absorption property has still limited lignin-containing paper from being desirable light management material that can transfer and manage visible light for optical engineering applications. Chromophore groups include conjugated double bonds, carbonyl groups, quinone groups, and free radicals, and autochrome groups, such as phenolic hydroxyl groups, hydroxyl groups, and carboxyl groups, are the main contributors to the color and light absorption of lignin. Jiang et al have reported the removal of lignin chromophores in lignocellulose nanofibrils using an alkaline-H_2O_2 hydrothermal method without significantly affecting the bulk lignin structure and content (Jiang et al., 2020). The resulting lignin-modified LNPs exhibited a comparable optical transmittance (~90%) but superior UV-shielding and water-resistant performances compared with CNPs, which was attributed to the well-preserved lignin structures. Moreover, such a transparent LNP was demonstrated to be a suitable light-management material that can significantly improve the power conversion efficiency of a GaAs solar cell. However, the alkaline-H_2O_2 hydrothermal strategy for fabricating transparent LNPs still involves intensive chemical reactions and water and energy consumption. The high reactivity of the photoexcited chromophoric radicals can contribute to an efficient and fast photocatalytic degradation process for chromophores to obtain a whitened lignin. Several photocatalytic methods, such as H_2O_2/UV (Qiu et al., 2018), TiO_2/H_2O_2/UV (Gupta et al., 2012), and Fe^{2+}/H_2O_2/UV (Lucas & Peres, 2006), have been reported for the discoloration of colored organic materials. Wang et al. achieved a fast decolorization rate for alkali lignin by using a combined THF/UV treatment, which can also be applied to the bleaching of raw paper (Wang et al., 2016). Xia et al. (2021) modified/decolorized lignin in wood in situ through a UV-assisted H_2O_2 oxidation strategy for the scalable and rapid manufacturing of transparent wood Click or tap here to enter text.. Park et al. (2020) have reported peracetic acid treatment to remove lignin chromophore with acetic acid, and hydrogen peroxide was directly mixed at a ratio of 4:1, 1:1, and 1:4 (v/v) and employed as reaction media at 80 ^oC.

Herein, a semi-transparent composite film from rice straw-based microfibrillated cellulose and chitosan (MFC/CS) was prepared successfully for light management application. The lignin-containing MFC was synthesized via a green and scalable method, which used dilute NaOH solution at 60 ^oC, 5000 rpm on a homogenizer, and neutralized with dilute HCl solution. The lignin on MFC was followed by peracetic acid treatment with H_2O_2 and acetic acid (ratio 4: 1 v/v) at 80^o C. The wastewater from this method is dilute NaCl solution (1.4 wt%), which minimizes the environmental impact. The MFC/CS composite

films were prepared by a simple blending method. The composite film exhibits an acceptable transparent and strong diffusing effect, making it suitable for light management applications.

2. Experiment

2.1. Materials

Rice straws were collected from local sources. The collected rice straws were chopped into pieces 2 mm in length, followed by prewashing and drying before further treatment. Chitosan (medium molecular weight, 75-85% deacetylated), vanillin (99%), hydroperoxide (H_2O_2, 30%), acetic acid (CH_3COOH, 99%), hydrochloric acid (HCl, 35%), and sodium hydroxide (NaOH, 97%) were purchased from Sigma Aldrich. All chemicals have been used as received without any further purification. Deionized water (DIW) was used in all experiments.

2.2. Preparation of microfibrillated cellulose (MFC) and modification of lignin

Two grams of chopped rice straw was added into 100 mL aqueous NaOH solution 0.5 wt%. The mixture was stood for 15 minutes and then stirred at 5000 rpm using a high flex homogenizer (HF91, SMT) at 60 ^oC for one hour. Afterward, the reaction mixture was cooled to room temperature and neutralized with an aqueous HCl solution of 1 wt%. The mixture was then added with 12 mL of H_2O_2 30% and 3 mL of glacial acetic acid (the volume ratio of H_2O_2/acetic acid is 4:1). The mixture was heated to 60 ^oC for 12 h and stood at room temperature for another 12 h. The mixture was then filtered and washed thoroughly with DIW. The wet MFC was calculated solid content and stored in the fridge at 4^o C for further use. A schematic illustration of the preparation of modified lignin on microfibrillated cellulose is shown in Figure 1.

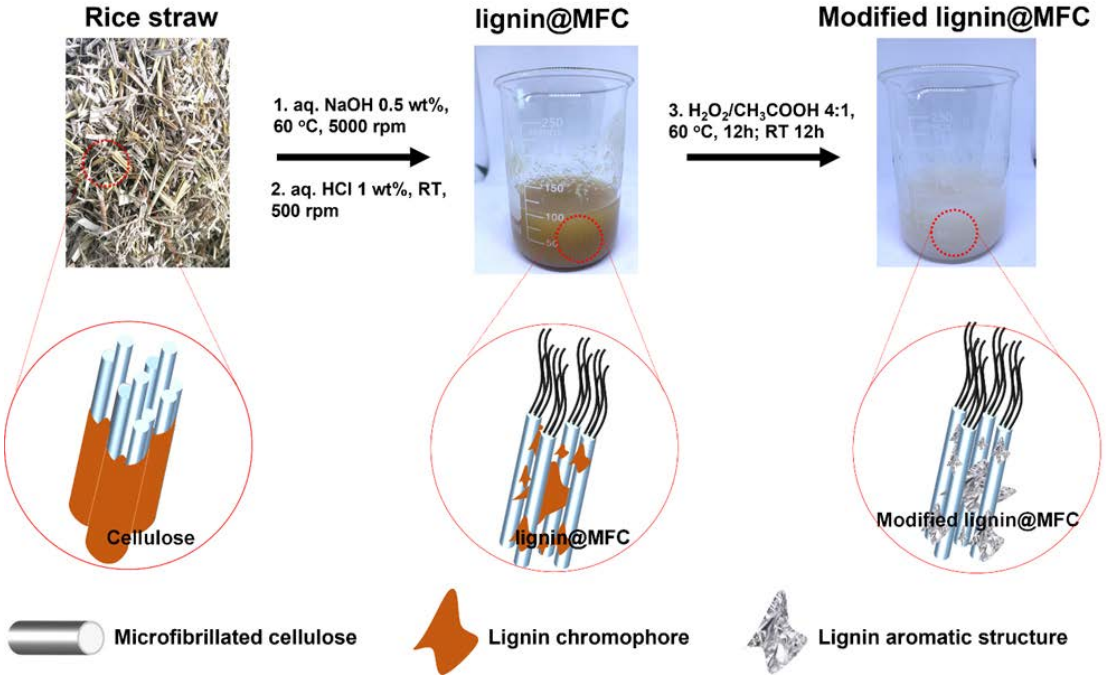

Figure 1. *Schematic illustration of a green method for preparation of lignin-modified MFC*

2.3. Preparation of CS/MFC solution and composite films

1g of CS was dissolved in 100 mL aqueous acetic solution 5 wt%. The calculated amounts of MFC were added to the CS solution to obtain a mixture with MFC/CS weight ratios of 1:3, 1:1, and 3:1, which are named MFC1/CS3, MFC1/CS1, and MFC3/CS1, respectively. The mixtures were then stirred at 5000 rpm using a high flex homogenizer (HF91, SMT) at room temperature for 30 min to obtain a well-dispersed solution. The CS, MFC, and composite films were prepared from the dispersion using a heating bar coating machine at 60^o C.

2.4. Characterizations

The morphology of the samples was observed using a scanning electron microscope (SEM) (JSM-6010PLUS, JEOL) operated at 11 kV accelerating voltage. The samples were coated with platinum for 30 s at 15 mA. The tensile strength of the films was investigated using a benchtop tensile strength tester (AI-1000-U, GOTECH) with 100N loadcell and strain rate of 10 mm/min. All tensile samples were cut into 8 mm x 60 mm rectangle shapes with thicknesses of 40-80 μm. The viscosities of all mixtures were determined using a digital viscometer (DV1, Brookfield) with LV-03 spindle at a speed of 100 rpm for CS solution and CS/MFC dispersion and LV-01 spindle at a speed of 20 rpm for MFC dispersion. The transmittance and absorbance of the films were evaluated on a UV-Vis spectrometer (USB2000+, OCEAN OPTICS) equipped with a UV-Vis light source (CHEM2000-UV-Vis, 190-850 nm). The light intensity was investigated using a digital lux meter (ST9620, SMART SENSOR).

3. Results and discussion

The chitosan concentration was fixed at 0.01 g/mL, and MFC was added to the chitosan solutions with weight ratios of MFC to chitosan 1:3, 1:1, and 3:1 to investigate the stability of MFC in the chitosan solution. The intense interaction between chitosan and MFC through hydrogen bonding was expected to give high stability of MFC dispersion, enabling the processing of uniform composite film (Wang et al., 2017; Zhang et al., 2022). The photographs of MFC and MFC/CS suspensions were prepared after 24 h and 48 h shown in Figure 2. After 24 h, MFC precipitation was found in MFC suspension, but no phase separation was found in three MFC/CS suspensions. The excellent stability implies that the presence of CS can enhance the dispersion of MFC suspension. However, after 48 h, the phase separation can be observed in MFC1/CS3 and MFC3/CS1. In MFC1/CS3, the dispersion viscosity is low, leading to weak interaction of MFC to CS solution phase. Thus, the precipitation of MFC can be observed. In MFC3/CS1, the amount of CS is insufficient to encapsulate the MFC surface to prevent aggregation of MFCs resulting in phase separation. The sample MFC/CS 1:1 showed excellent dispersion behavior; thus, this composition is expected to give uniform dispersion of MFC in the dried composite film.

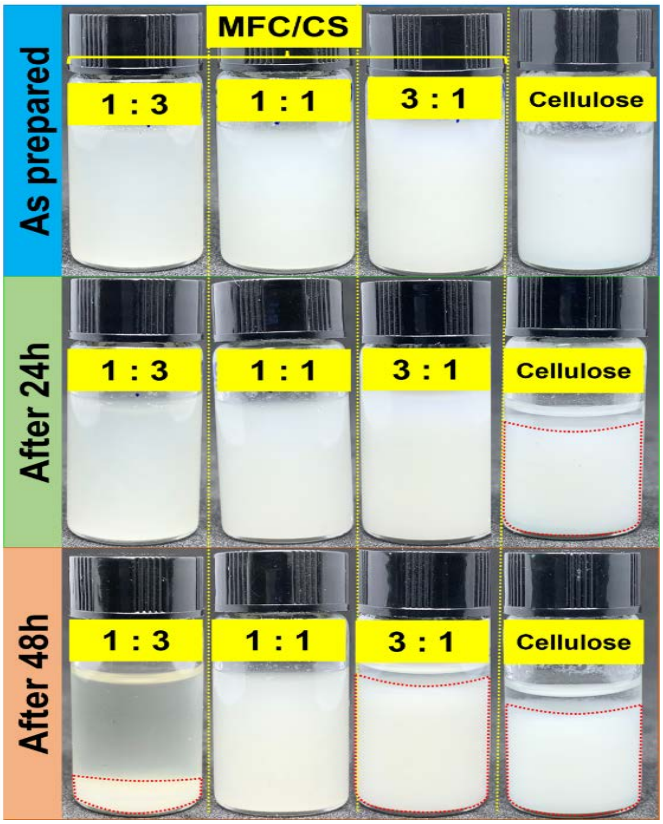

Figure 2. *Dispersion stabilities as-prepared after 24 h and 48 h*

The rheology of the MFC/CS suspensions was further investigated using a viscometer. The viscosities of CS and MFC/CS as a function of times are shown in Figure 3a. The viscosity value in the 30 s is shown in Figure 3b as a function of MFC/CS weight ratios. The viscosity of three MFC/CS dispersions is stable for up to 60 s, implying that well dispersion of MFC in the mixture. The fungal-like adhesive materials between CS and MFC have been reported (Sanandiya et al., 2018) thanks to strong hydrogen bonding between amino groups on CS and hydroxy groups on MFCs. A significant decrease of viscosity from 403 cP in CS solution 0.01 g/mL to 269 cPs with adding MFC of 0.0033 g/mL in MFC1/CS3 was found. This decrease with adding MFC can be attributed to the extraction of CS to MFC surfaces leading to a reduction of free CS in the solution. At higher MFC concentrations in MFC1/CS1 and MFC3/CS1, the concentrations of MFC are high enough to form floc structure leading to an increase of viscosity to 370 cPs and 379 cPs, respectively.

Figure 3c shows the tensile strength of CS and composite films. The CS film exhibits high ductile behavior with maximum stress and elongation at a break of 24.1 MPa and 18.8%, respectively. Adding a low concentration of MFC in MFC1/CS3 means the maximum stress and elongation at break are 11.7 MPa and 7.1%. The MFC1/CS3 exhibits the highest stiffness with a maximum stress of 56.6% and elongation at a break of 4.4%. The MFC1/CS3 shows the lowest stress and elongation at break, which is 8.1 MPa and 4.7%, respectively. Figure 3d-**f** shows SEM images of CS film, MFC on a silicon wafer, MFC film,

and composite films. The insets show their cross-sectional SEM images. The SEM image of CS shows a smooth surface with a high uniform thickness of the film. Figure 3e-f show that the MFC has variation in diameter in the range of 2-5 μm and length up to 200 μm. Figure 3g-i clearly shows CS coverage on MFC, which causes an increase in MFC diameter to the range of 5-10 μm. The SEM images of all composite films show excellent adhesion between the CS matrix and MFC, with no clear interface found in all samples. The inserted cross-sectional images of MFC1/CS3 and MFC1/CS1 films exhibit uniform MFC in the film, whereas MFC3/CS1 shows MFC's phase separation and precipitation at the film's bottom. This phase separation explains the reason for the worst mechanical properties of the MFC3/CS1 film, as discussed in **Figure 3c**.

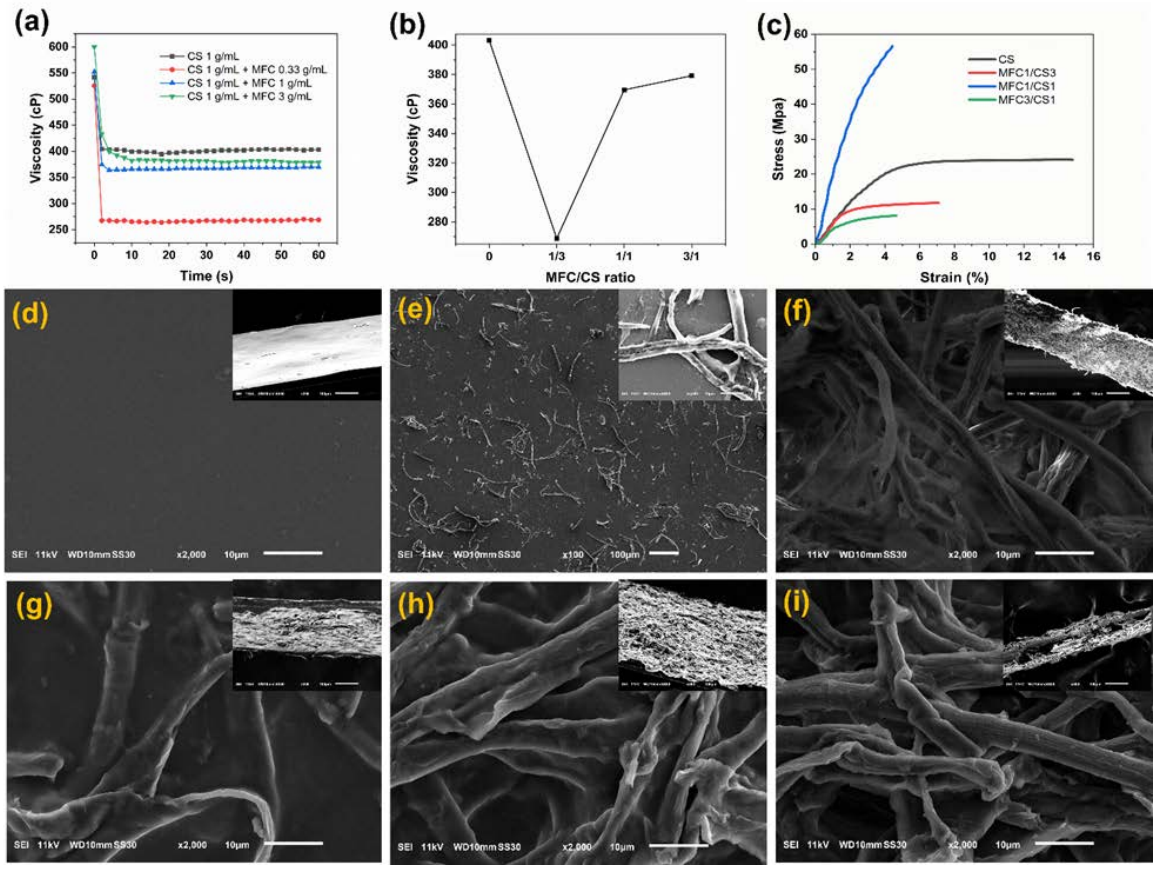

Figure 3. *(a) viscosity of dispersions; (b) viscosity as a function of MFC/CS ratios; (c) stress-strength curves of CS and composite films; (d-i) SEM images: (d) CS, (e) MFC on a silicon wafer, (f) MFC film, (g) MFC1/CS3 film, (h) MFC1/CS1 film, (i) MFC3/CS1 film. The insets are cross-sectional views*

Figure 4a presents the transparency of CS and composite films with thickness in a range of 51.8 to 58.4 μm. The MFC1/CS3 and MFC1/CS1 films exhibit quite good clarity compared to neat CS films. The MFC3/CS1 and MFC are opaque films. Figure 4b shows the transmittance and absorbance of CS, MFC1/CS3, and MFC1/CS1 films. Interestingly,

although MFC1/CS3 and MFC1/CS1 exhibit comparable visual transparency to CS film, they have much lower transmittance than neat CS film, which are 58.5%, 2.4%, and 0.8% for CS, MFC1/CS3, and MFC1/CS1, respectively. While CS film shows an absorbance peak in a range of 230 to 400 nm and transmitted the rest range of wavelength, the MFC1/CS3 and MFC1/CS1 exhibit high absorbance full range of investigated wavelength from 230 to 850 nm. This improvement implies that composite film with MFC can provide diffusing effects, as reported for nanocellulose fiber (NFC) (Jiang et al., 2022) and transparent wood (K. Wang, Zhang, et al., 2022; Xia, Chen, Li, et al., 2021) for light management applications. To visualize diffusing phenomenon of MFC1/CS3 and MFC1/CS1 composite films. In the system in Figure 4c, the green laser beam illuminates the CS and composite film at 5 cm, and all passing lights are collected using a black screen at a distance of 5 cm from the film. Figure 4d show a focused laser beam on the screen. With inserted CS film, the collected passing lights show scattering by crystalline domains of CS (Figure 4e). With MFC1/CS3, the diffused and broadening light beam was observed. However, it is clear to see two regions, including strong light density at the center and diffused light outer (Figure 4f). With MFC1/CS1, the focused light beam is disappeared, and the lights become more uniform (Figure 4g).

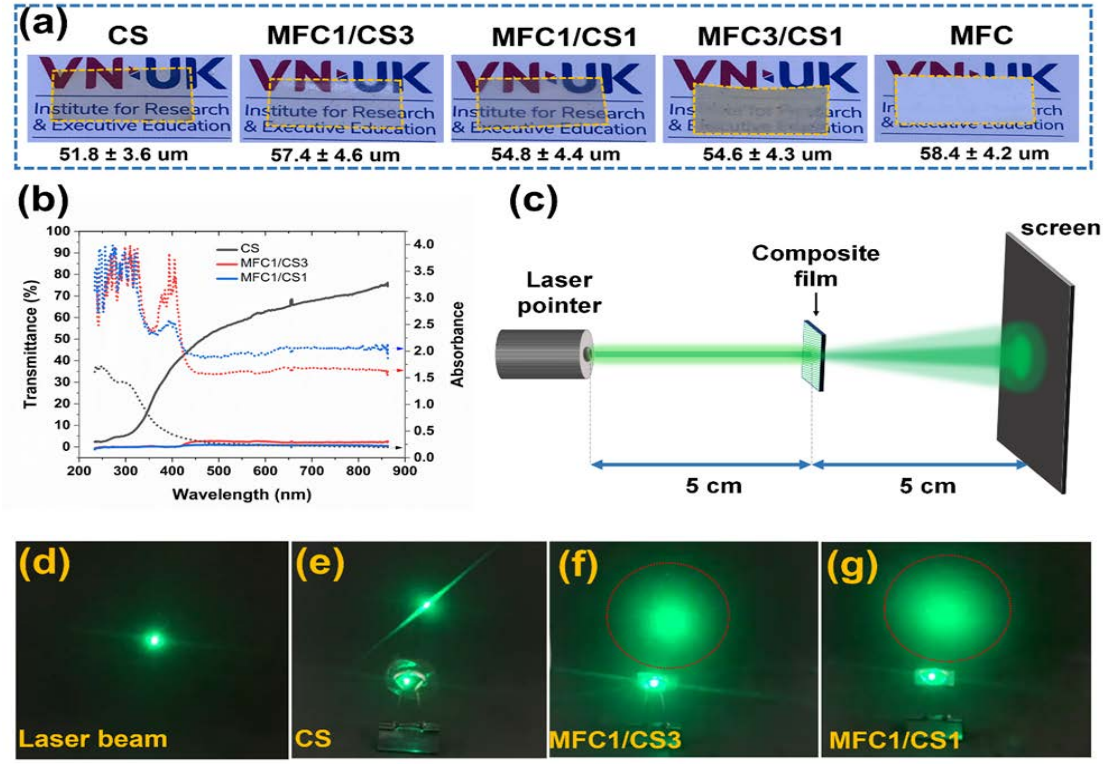

Figure 4. *(a) visual transparency of CS and composite films; (b) transmittance and absorbance of CS, MFC1/CS3, MFC1/CS1 films; (c) apparatus to visualize diffusing of the laser beam by applying composite films; (d-f) diffusing of laser beam: (d) without film, (e) CS film, (f) MFC1/CS3 film, (g) MFC1/CS1 film*

To evaluate the capability of composite film to control light intensity for light management applications. As shown in Figure 5a, an apparatus was set up in which the green laser pointer was set at a fixed distance to a digital Lux meter at 11 cm. The composite films were put between a laser pointer and a digital Lux meter, changing lengths from the film to the digital Lux meter from 1 to 10 cm. The percentage decrease of light intensity as a function of the distance between film to digital Lux meter was plotted in Figure 5b. The light intensity decreases with increasing distance between film to Lux sensor in CS, MFC1/CS3, and MFC1/CS1 films. While the CS exhibits a decrease of light intensity from 90.6% to 78.9% for distance change from 1 to 10 cm, the values for MFC1/CS3 and MFC1/CS1 are 78.3% to 15.1% and 67.9% to 7.9%, respectively. The MFC1/CS1 provides a more diffusing effect than MFC1/CS1, with a lower value in light intensity at the exact distances. The results proved that MFC1/CS3 and MFC1/CS1 prevent sufficient direct sunlight and diffuse the light more uniformly in indoor spaces in the light management application.

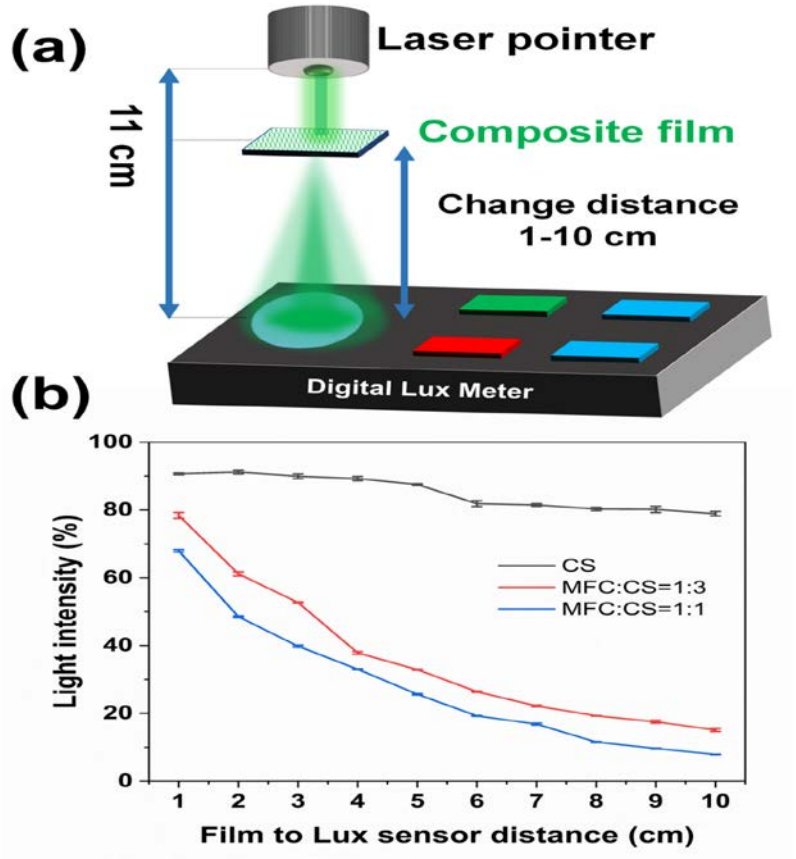

Figure 5. *(a) Apparatus set up for light intensity measurement; (b) Plot of light intensity change with changing distance between films and Lux detector*

The demonstration used composite film for light management applications. A 6 cm x 8 cm of MFC1/CS1 was fabricated with a frame as a model of a window (Figure 6a). A commercial flashlight was set at 1 m to the floor. By applying the composite film at a distance of 0.5 m to the flashlight, the diffusing light can be magnified up to more than four

times the diameter of the original light (Figure 6b-c). Figure 6d illustrates that focusing sunlight through a window causes high light intensity on a small floor region. By applying composite film to a window, as in Figure 6e, the sunlight can be diffused uniformly everywhere in the room.

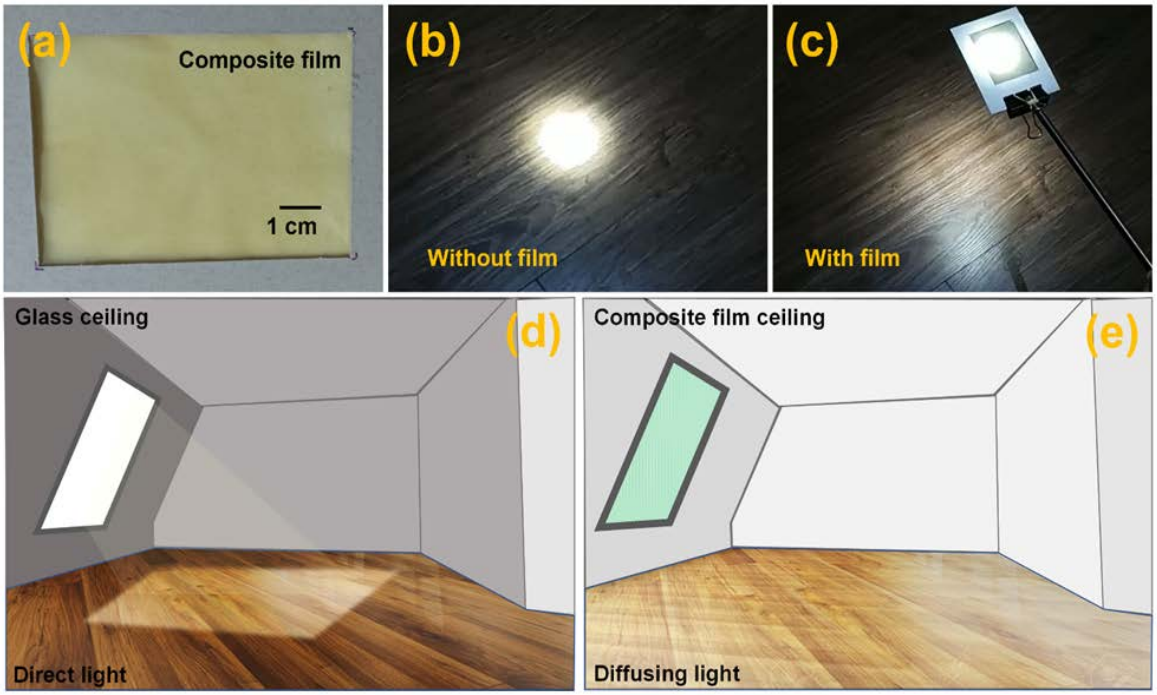

Figure 6. *(a) photograph of 6 cm x 8 cm MFC1/CS1 composite film; (b-c) diffusing flashlight without and with composite film; (d-e) illustration of a glass ceiling and composite film ceiling in promoting effective sunlight harvesting and offering comfortable indoor lighting*

4. Conclusion

This work demonstrates a simple and green strategy to fabricate MFC/CS composite film for light management applications. Lignin-modified MFC was synthesized successfully via a scalable method using a combination of hydroperoxide and acetic acid. The composite film showed good transparency and excellent diffusing effects, which can be large-scale in roll-to-roll technology. Thus, the composite is a promising candidate for light management to increase the energy efficiency of buildings.

❖ ***Conflict of Interest:*** *Authors have no conflict of interest to declare.*

❖ ***Acknowledgement:*** *This research is funded by the People's Committee of Da Nang city.*

REFERENCES

Abuelnuor, A. A. A., Omara, A. A. M., Saqr, K. M., & Elhag, I. H. I. (2018). Improving indoor thermal comfort by using phase change materials: A review. *International Journal of Energy Research*, *42*(6), 2084-2103. https://doi.org/10.1002/er.4000

Ascione, F., Bianco, N., Iovane, T., Mastellone, M., & Mauro, G. M. (2021). The evolution of building energy retrofit via double-skin and responsive façades: A review. *Solar Energy*, *224*(June), 703–717. https://doi.org/10.1016/j.solener.2021.06.035

Breyer, C. (2020). A Global Overview of Future Energy. In *Future Energy* (pp. 727-756). Elsevier. https://doi.org/10.1016/B978-0-08-102886-5.00034-7

Djafari Petroudy, S. R., Rahmani, N., Rasooly Garmaroody, E., Rudi, H., & Ramezani, O. (2019). Comparative study of cellulose and lignocellulose nanopapers prepared from hardwood pulps: Morphological, structural and barrier properties. *International Journal of Biological Macromolecules*, *135*, 512-520. https://doi.org/10.1016/j.ijbiomac.2019.05.212

Dong, Y., Tan, Y., Wang, K., Cai, Y., Li, J., Sonne, C., & Li, C. (2022). Reviewing wood-based solar-driven interfacial evaporators for desalination. *Water Research*, *223*, 119011. https://doi.org/10.1016/J.WATRES.2022.119011

Eh, A. L. S. S., Tan, A. W. M., Cheng, X., Magdassi, S., & Lee, P. S. (2018). Recent Advances in Flexible Electrochromic Devices: Prerequisites, Challenges, and Prospects. *Energy Technology*, *6*(1), 33-45. https://doi.org/10.1002/ente.201700705

Eyl-Mazzega, M.A., & Mathieu, C. (2020). The European Union and the Energy Transition. In *Lecture Notes in Energy* (Vol. 73, pp. 27-46). https://doi.org/10.1007/978-3-030-39066-2_2

Fang, Z., Li, G., Hou, G., & Qiu, X. (2023). *Light Management of Nanocellulose Films*. 179-209. https://doi.org/10.1007/978-3-031-14043-3_6

Gupta, V. K., Jain, R., Mittal, A., Saleh, T. A., Nayak, A., Agarwal, S., & Sikarwar, S. (2012). Photo-catalytic degradation of toxic dye amaranth on TiO2/UV in aqueous suspensions. *Materials Science and Engineering: C*, *32*(1), 12-17. https://doi.org/10.1016/j.msec.2011.08.018

Jiang, Y., Liu, X., Yang, Q., Song, X., Qin, C., Wang, S., & Li, K. (2019). Effects of residual lignin on composition, structure, and properties of mechanically defibrillated cellulose fibrils and films. *Cellulose*, *26*(3), 1577-1593. https://doi.org/10.1007/s10570-018-02229-4

Jiang, Y., Wang, Z., Liu, X., Yang, Q., Huang, Q., Wang, L., Dai, Y., Qin, C., & Wang, S. (2020). Highly Transparent, UV-Shielding, and Water-Resistant Lignocellulose Nanopaper from Agro-Industrial Waste for Green Optoelectronics. *ACS Sustainable Chemistry & Engineering*, *8*(47), 17508-17519. https://doi.org/10.1021/acssuschemeng.0c06752

Jiang, Y., Wang, Z., Zhou, L., Jiang, S., Liu, X., Zhao, H., Huang, Q., Wang, L., Chen, G., & Wang, S. (2022). Highly efficient and selective modification of lignin towards optically designable and multifunctional lignocellulose nanopaper for green light-management applications. *International Journal of Biological Macromolecules*, *206*(January), 264-276. https://doi.org/10.1016/j.ijbiomac.2022.02.147

Lee, J., & Yang, J.-S. (2019). Global energy transitions and political systems. *Renewable and Sustainable Energy Reviews*, *115*(August), 109370. https://doi.org/10.1016/j.rser.2019.109370

Li, T., Chen, C., Brozena, A. H., Zhu, J. Y., Xu, L., Driemeier, C., Dai, J., Rojas, O. J., Isogai, A., Wågberg, L., & Hu, L. (2021). Developing fibrillated cellulose as a sustainable technological material. *Nature*, *590*(7844), 47-56. https://doi.org/10.1038/s41586-020-03167-7

Lizundia, E., Sipponen, M. H., Greca, L. G., Balakshin, M., Tardy, B. L., Rojas, O. J., & Puglia, D. (2021). Multifunctional lignin-based nanocomposites and nanohybrids. *Green Chemistry*, *23*(18), 6698-6760. https://doi.org/10.1039/D1GC01684A

Lucas, M., & Peres, J. (2006). Decolorization of the azo dye Reactive Black 5 by Fenton and photo-Fenton oxidation. *Dyes and Pigments*, *71*(3), 236-244. https://doi.org/10.1016/j.dyepig.2005.07.007

Mariano-Hernández, D., Hernández-Callejo, L., Zorita-Lamadrid, A., Duque-Pérez, O., & Santos García, F. (2021). A review of strategies for building energy management system: Model predictive control, demand side management, optimization, and fault detect & diagnosis. *Journal of Building Engineering*, *33*, 101692. https://doi.org/10.1016/j.jobe.2020.101692

Mi, R., Chen, C., Keplinger, T., Pei, Y., He, S., Liu, D., Li, J., Dai, J., Hitz, E., Yang, B., Burgert, I., & Hu, L. (2020). Scalable aesthetic transparent wood for energy efficient buildings. *Nature Communications*, *11*(1), 3836. https://doi.org/10.1038/s41467-020-17513-w

Mohelnikova, J. (2011). Nanocoatings for architectural glass. In *Nanocoatings and Ultra-Thin Films* (pp. 182-202). Elsevier. https://doi.org/10.1533/9780857094902.2.182

Oliaei, E., Lindén, P. A., Wu, Q., Berthold, F., Berglund, L., & Lindström, T. (2020). Microfibrillated lignocellulose (MFLC) and nanopaper films from unbleached kraft softwood pulp. *Cellulose*, *27*(4), 2325-2341. https://doi.org/10.1007/s10570-019-02934-8

Park, S.-Y., Choi, J. H., Kim, J.-H., Cho, S. M., Yeon, S., Jeong, H., Lee, S. M., & Choi, I. G. (2020). Peracetic acid-induced kraft lignin solubilization and its characterization for selective production of macromolecular biopolymers. *International Journal of Biological Macromolecules*, *161*, 1240–1246. https://doi.org/10.1016/j.ijbiomac.2020.06.041

Pereira, J., Glória Gomes, M., Moret Rodrigues, A., & Almeida, M. (2019). Thermal, luminous and energy performance of solar control films in single-glazed windows: Use of energy performance criteria to support decision making. *Energy and Buildings*, *198*, 431-443. https://doi.org/10.1016/j.enbuild.2019.06.003

Pereira, J., Teixeira, H., Gomes, M. da G., & Moret Rodrigues, A. (2022). Performance of Solar Control Films on Building Glazing: A Literature Review. *Applied Sciences*, *12*(12), 5923. https://doi.org/10.3390/app12125923

Qiu, X., Yu, J., Yang, D., Wang, J., Mo, W., & Qian, Y. (2018). Whitening Sulfonated Alkali Lignin via H 2 O 2 /UV Radiation and Its Application As Dye Dispersant. *ACS Sustainable Chemistry & Engineering*, *6*(1), 1055-1060. https://doi.org/10.1021/acssuschemeng.7b03369

Rashidi, S., Esfahani, J. A., & Karimi, N. (2018). Porous materials in building energy technologies—A review of the applications, modelling and experiments. *Renewable and Sustainable Energy Reviews*, *91*(September 2017), 229-247. https://doi.org/10.1016/j.rser.2018.03.092

Sanandiya, N. D., Vijay, Y., Dimopoulou, M., Dritsas, S., & Fernandez, J. G. (2018). Large-scale additive manufacturing with bioinspired cellulosic materials. *Scientific Reports*, *8*(1), 8642. https://doi.org/10.1038/s41598-018-26985-2

Song, M., Niu, F., Mao, N., Hu, Y., & Deng, S. (2018). Review on building energy performance improvement using phase change materials. *Energy and Buildings*, *158*, 776-793. https://doi.org/10.1016/j.enbuild.2017.10.066

Sun, J., Schütz, U., Tu, K., Koch, S. M., Roman, G., Stucki, S., Chen, F., Ding, Y., Yan, W., Wu, C., Stricker, L., Burgert, I., Wang, Z. L., Hegemann, D., & Panzarasa, G. (2022). Scalable and sustainable wood for efficient mechanical energy conversion in buildings via triboelectric effects. *Nano Energy*, *102*, 107670. https://doi.org/10.1016/J.NANOEN.2022.107670

Sun, Y., Wilson, R., & Wu, Y. (2018). A Review of Transparent Insulation Material (TIM) for building energy saving and daylight comfort. *Applied Energy*, *226*(May), 713-729. https://doi.org/10.1016/j.apenergy.2018.05.094

Tällberg, R., Jelle, B. P., Loonen, R., Gao, T., & Hamdy, M. (2019). Comparison of the energy saving potential of adaptive and controllable smart windows: A state-of-the-art review and simulation studies of thermochromic, photochromic and electrochromic technologies. *Solar Energy Materials and Solar Cells*, *200*(June 2018), 109828. https://doi.org/10.1016/j.solmat.2019.02.041

Wang, J., Deng, Y., Qian, Y., Qiu, X., Ren, Y., & Yang, D. (2016). Reduction of lignin color via one-step UV irradiation. *Green Chemistry*, *18*(3), 695-699. https://doi.org/10.1039/C5GC02180D

Wang, K., Liu, X., Dong, Y., Ling, Z., Cai, Y., Tian, D., Fang, Z., & Li, J. (2022). Editable shape-memory transparent wood based on epoxy-based dynamic covalent polymer with excellent optical and thermal management for smart building materials. *Cellulose*, *29*(14), 7955-7972. https://doi.org/10.1007/S10570-022-04754-9/TABLES/1

Wang, K., Peng, H., Gu, Q., Zhang, X., Liu, X., Dong, Y., Cai, Y., Li, Y., & Li, J. (2023). Scalable, large-size, and flexible transparent bamboo. *Chemical Engineering Journal*, *451*, 138349. https://doi.org/10.1016/J.CEJ.2022.138349

Wang, K., Zhang, T., Li, C., Xiao, X., Tang, Y., Fang, X., Peng, H., Liu, X., Dong, Y., Cai, Y., Tian, D., Li, Y., & Li, J. (2022). Shape-reconfigurable transparent wood based on solid-state plasticity of polythiourethane for smart building materials with tunable light guiding, energy saving, and fire alarm actuating functions. *Composites Part B: Engineering*, *246*, 110260. https://doi.org/10.1016/J.COMPOSITESB.2022.110260

Wang, Y., Uetani, K., Liu, S., Zhang, X., Wang, Y., Lu, P., Wei, T., Fan, Z., Shen, J., Yu, H., Li, S., Zhang, Q., Li, Q., Fan, J., Yang, N., Wang, Q., Liu, Y., Cao, J., Li, J., & Chen, W. (2017). Multifunctional Bionanocomposite Foams with a Chitosan Matrix Reinforced by Nanofibrillated Cellulose. *ChemNanoMat*, *3*(2), 98-108. https://doi.org/10.1002/cnma.201600266

Wang, Z., Wang, X., Cong, S., Geng, F., & Zhao, Z. (2020). Fusing electrochromic technology with other advanced technologies: A new roadmap for future development. *Materials Science and Engineering: R: Reports*, *140*(2020), 100524. https://doi.org/10.1016/j.mser.2019.100524

Xia, Q., Chen, C., Li, T., He, S., Gao, J., Wang, X., & Hu, L. (2021). Solar-assisted fabrication of large-scale, patternable transparent wood. *Science Advances*, *7*(5), 1-9. https://doi.org/10.1126/sciadv.abd7342

Xia, Q., Chen, C., Yao, Y., Li, J., He, S., Zhou, Y., Li, T., Pan, X., Yao, Y., & Hu, L. (2021). A strong, biodegradable and recyclable lignocellulosic bioplastic. *Nature Sustainability*, *4*(7), 627-635. https://doi.org/10.1038/s41893-021-00702-w

Yang, X., Abe, K., Yano, H., & Wang, L. (2022). Multifunctional cellulosic materials prepared by a reactive DES based zero-waste system. *Nano Letters*, *22*(15), 6128-6134. https://doi.org/10.1021/ACS.NANOLETT.2C01303/SUPPL_FILE/NL2C01303_SI_002.PDF

Zhang, Y., Wei, Y., Qian, Y., Zhang, M., Zhu, P., & Chen, G. (2020). Lignocellulose enabled highly transparent nanopaper with tunable ultraviolet-blocking performance and superior durability. *ACS Sustainable Chemistry and Engineering*, *8*(46), 17033-17041. https://doi.org/10.1021/acssuschemeng.0c04145

Zhang, Y., Yang, S., Tang, H., Wan, S., Qin, W., Zeng, Q., Huang, J., Yu, G., Feng, Y., & Li, J. (2022). Depletion stabilization of emulsions based on bacterial cellulose/carboxymethyl chitosan complexes. *Carbohydrate Polymers*, *297*(July), 119904. https://doi.org/10.1016/j.carbpol.2022.119904

Zhao, D., Zhu, Y., Cheng, W., Chen, W., Wu, Y., & Yu, H. (2021). Cellulose-Based Flexible Functional Materials for Emerging Intelligent Electronics. *Advanced Materials*, *33*(28), 2000619. https://doi.org/10.1002/adma.202000619

MÀNG COMPOSITE BÁN TRONG SUỐT TỔNG HỢP TỪ VI SỢI CELLULOSE CÓ NGUỒN GỐC RƠM RẠ NGHIỀN NHỎ VÀ ỨNG DỤNG TRONG KIỂM SOÁT ÁNH SÁNG

Trần Văn Khuê[1], Lê Văn Thuận[2,3], Nguyễn Minh Hiệp[4], Đặng Ngọc Sỹ[5], Đoàn Minh Thu[1], Lê Hoàng Sinh[1,2*]

[1]Viện Nghiên cứu và Đào tạo Việt – Anh, Đại học Đà Nẵng, Việt Nam
[2]Trung tâm Hóa học Tiên tiến, Viện Nghiên cứu và Phát triển Công nghệ cao, Trường Đại học Duy Tân, Việt Nam
[3]Khoa Khoa học Tự nhiên, Trường Đại học Duy Tân, Việt Nam
[4]Trung tâm Công nghệ Bức xạ và Công nghệ Sinh học, Viện Nghiên cứu Hạt nhân, Đà Lạt, Việt Nam
[5]Trung tâm Kỹ thuật Cơ khí, Trường Đại học Duy Tân, Việt Nam
[*]Tác giả liên hệ: Lê Hoàng Sinh – Email: sinh.le@vnuk.edu.vn

Ngày nhận bài: 11-10-2022; ngày nhận bài sửa: 08-11-2022; ngày duyệt đăng: 30-12-2022

TÓM TẮT

Màng composite bán trong suốt từ cellulose và chitosan (MFC/CS) được nghiền nhỏ dựa trên rơm rạ đã được chứng minh là một vật liệu kiểm soát sự truyền qua của ánh sáng mở ra hướng ứng dụng đầy hứa hẹn trong các kĩ thuật quang học thế hệ tiếp theo. Trong bài báo này, một phương pháp xanh tổng hợp MFC được bao phủ bởi lignin đã được phát triển thành công, trong đó MFC lần đầu tiên được chiết xuất bằng cách sử dụng dung dịch natri hydroxit loãng trên thiết bị đồng hóa ở tốc độ 5000 vòng/phút. Lignin hòa tan sau đó được lắng đọng trên bề mặt MFC sau khi trung hòa natri hydroxit bằng dung dịch axit clohydric loãng. MFCs thu được có đường kính từ 2-5 μm và chiều dài lên đến 200 μm. Lignin được khử màu bằng cách loại bỏ các nhóm mang màu của nó (chromophore groups) bằng axit peracetic với hỗn hợp hydro peroxit và axit axetic ở tỉ lệ thể tích 4: 1. Màng MFC cho thấy độ trong suốt cao và hiệu ứng phân tán ánh sáng tuyệt vời với tỉ lệ trọng lượng MFC/CS là 1: 3 và 1: 1.

Từ khóa: phương pháp xanh; kiểm soát ánh sáng; vi sợi cellulose, rơm rạ